Interwall interaction and electronic structure of double-walled BN nanotubes

Susumu Okada,[1] Susumu Saito,[2] and Atsushi Oshiyama[1]
[1]*Institute of Physics, University of Tsukuba, Tennodai, Tsukuba 305-8571, Japan*
and Center for Computational Physics, University of Tsukuba, Tennodai, Tsukuba 305-8577, Japan
[2]*Department of Physics, Tokyo Institute of Technology, 2-12-1 Oh-okayama, Meguro-ku, Tokyo 152-8551, Japan*
and Institute for Molecular Science, Myodaiji, Okazaki 444-8585, Japan
(Received 5 November 2001; published 4 April 2002)

We report first-principles total-energy electronic-structure calculations that provide energetics and electronic structures of double-walled BN nanotubes, $(n,0)$@(15,0) and $(m,0)$@(20,0). We find that the most favorable double-walled nanotubes studied here are (7,0)@(15,0) and (12,0)@(20,0) in which the interwall distances are about 3 Å. The electronic energy bands around the Fermi energy depend interestingly on the tube radii due to the hybridization between σ and π states. We also find that the nearly-free-electron states of the nanotubes induce peculiar charge redistribution in the interwall region.

DOI: 10.1103/PhysRevB.65.165410 PACS number(s): 71.20.Tx, 73.22.−f, 73.20.At

Following the discovery of carbon nanotubes,[1] similar forms of rolled honeycomb sheets consisting of boron and nitrogen atoms have been synthesized using the arc discharge[2,3] and substitution[4] techniques: Multiwalled BN nanotubes[2,3] (BN MWNT's) and single-walled BN nanotubes[5,6] (BN SWNT's) have been reported. An analysis of the electron-diffraction pattern on ropes of BN MWNT's reveals that most of the BN nanotubes possess zigzag [$(n,0)$ type] atomic arrangement along the tube circumference.[7] It is also found that the majority of the BN nanotubes are even walled.[7,8] Furthermore, the transmission electron microscope (TEM) clearly shows that there are certain atomic arrangements between each zigzag nanotube in the MWNT's (interwall stacking order).[9] The electronic structure of BN SWNT's is semiconducting with a moderate energy gap[10,11] due to the large energy gap of the honeycomb sheet of the BN (h-BN) and is entirely different from that of the single-walled carbon nanotubes (C SWNT's) whose electronic structure shows rich variety in a range from semiconductors to metals depending on their global network topology.[12,13] The electronic structure of BN MWNT's is, however, to our best knowledge, not known yet. In the BN MWNT's, the interwall interaction plays an important role for the stacking ordering of each tube. Thus the electronic states of BN MWNT's may also show interesting modulations which we will discuss in this paper.

We report here total-energy electronic-structure calculations performed for double-walled zigzag BN nanotubes (BN DWNT's). We take zigzag BN-DWNT's, $(n,0)$@(15,0) ($n=5$–9) and $(n,0)$@(20,0), ($n=10$–13) to clarify common characteristics of the energetics and electronic structures of BN MWNT's consisting of thin and thick nanotubes. We find that the (7,0) and (12,0) inner tubes are the most energetically favorable for the outer (15,0) and (20,0) tubes, respectively. The BN DWNT's studied here are direct-gap semiconductors exhibiting interesting variations of electronic states around the energy gap: The top of the valence and the bottom of the conduction bands are localized on the outer and inner nanotubes, respectively, due to particular hybridization between π and σ states of each tube. This peculiar character of MWNT's may be utilized in optoelectronic devices in the future.

All calculations have been performed using local-density approximation (LDA) in the density-functional theory.[14,15] It is known that the interlayer interactions of the graphite and h-BN are reproduced by using LDA. Thus LDA is an adequate approximation to examine the stability of BN DWNT's which is partially due to the interwall interaction between inner and outer nanotubes. For the exchange-correlation energy among electrons, we use a functional form[16] fitted to the Monte Carlo results for the homogeneous electron gas.[17] Norm-conserving pseudopotentials generated by using the Troullier-Martins scheme are adopted to describe the electron-ion interaction.[18,19] The valence wave functions are expanded by the plane-wave basis set with a cutoff energy of 50 Ry which gives enough convergence of relative total energies of h-BN.[20] We adopt a supercell model in which a DWNT is placed with its outer wall separated from another wall of an adjacent nanotube by 8.0 Å. The conjugate-gradient minimization scheme is utilized both for the electronic-structure calculation and for geometry optimization.[21] Integration over a one-dimensional Brillouin zone is carried out using the two k points. Convergence of the total energy with respect to the number of sampling k points is examined on the (7,0)@(15,0) BN NT by performing the computation with 2, 4, 6, 8, 10, and 11 k points. The total energy obtained with a two k points sampling is smaller by 0.005 eV/atom than that obtained with an 11 k points sampling.

Figure 1 shows the optimized geometries of BN DWNT's, (5,0)@(15,0), (7,0)@(15,0), (9,0)@(15,0), (10,0)@(20,0), and (12,0)@(20,0). In the DW NT's, (5,0)@(15,0) and

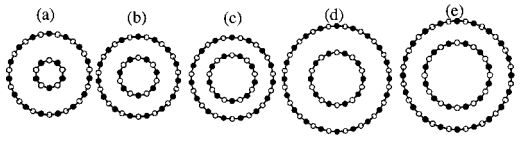

FIG. 1. Cross-sectional views of optimized geometries of (a) (5,0)@(15,0), (b) (7,0)@(15,0), (c) (9,0)@(15,0), (d) (10,0)@(20,0), and (e) (12,0)@(20,0) BN DWNT's. Open and solid circles denote the B and N atoms, respectively.

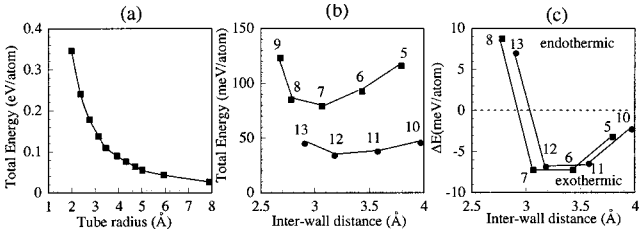

FIG. 2. (a) Total energy per atom of BN SWNT's as a function of the tube radius. (b) Total energy per atom and (c) formation energy per atom (ΔE) of each BN DWNT as a function of the interwall distance between inner and outer nanotubes. Solid squares and circles denote the total and formation energies of $(n,0)$@(15,0) DWNT's and $(m,0)$@(20,0) DWNT's, respectively. Indices of n and m are listed in the figures. The energies are measured from that of the h-BN.

(10,0)@(20,0), it is possible to place each B (or N) atom in the inner nanotube so as to face a N (or B) atom in the outer nanotube, leading to the AB stacking order between the inner and outer tubes as in the case of the hexagonal stacking in the h-BN solid. We assume this AB stacking for these tubes. On the other hand, the remaining DWNT's have AB stacking only in part of their walls. The structural relaxation causes small buckling on the tube circumference:[22] In all the optimized structures studied here, B atoms move inward but N atoms move outward. The magnitude of buckling of the inner tube is about 0.12 Å for (5,0), 0.09 Å for (7,0), and 0.04 Å for (9,0), which decreases with increasing tube radius. On the other hand, buckling of the outer (15,0) tube increases with decreasing intertube space. Owing to this buckling, each B atom forms a small facet with its adjacent three N atoms. The buckling was also found on the BN SWNT's. The calculated values of buckling of SWNT's are 0.21 Å, 0.14 Å, and 0.11 Å, for (5,0), (7,0), and (9,0), respectively. The magnitude of buckling of DWNT's is found to be smaller than that of the SWNT's, due to the interwall interaction between inner and outer nanotubes.

In the h-BN, it is known that the interlayer interaction between honeycomb BN sheets stabilizes the system in a layered structure with the appropriate interlayer distance.[23] In the BN DWNT's, interwall interaction is also expected to stabilize the system and determine the preferable interwall distance and atomic stacking arrangement. Thus, the peculiar correlation between the interwall distance and the total energy of the DWNT is expected to take place. We show the total energy of the optimized geometry of BN DWNT's and that of BN SWNT's in Figs. 2(a) and 2(b). The total energy of SWNT's decreases with increasing tube radius and gradually approaches that of the h-BN. On the other hand, the total energy of DWNT's has a local minimum around the interwall distance of about 3.0 Å. Thus, (7,0) and (12,0) are the preferable inner nanotubes for the (15,0) and (20,0) outer nanotubes, respectively. This stability is also corroborated by calculating the formation energy originated from the interwall interaction. Energy difference (ΔE) in the reaction, $(n,0)+(m,0)\rightarrow(n,0)@(m,0)-\Delta E$, is shown in Fig. 2(c). For the tubes thicker than the (7,0) for (15,0) and (12,0) for (20,0), double-walled structures cause energy loss and the

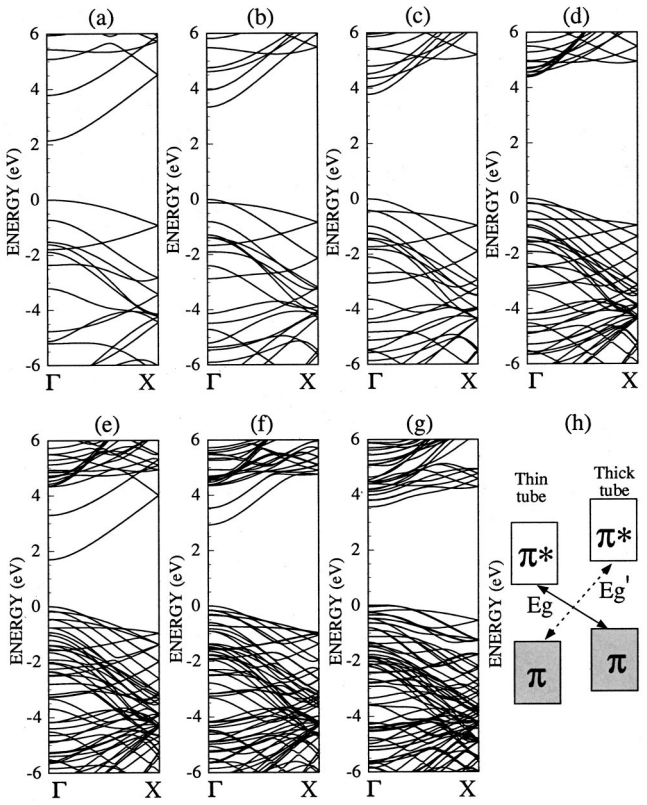

FIG. 3. Energy-band structure of (a) (5,0), (b) (7,0), (c) (9,0), and (d) (15,0) SWNT's. Energy band structure of DWNT $(n,0)$@(15,0) for (e) $n=5$, (f) $n=7$, and (g) $n=9$. Energies are measured from the top of the valence band. (h) An energy diagram of the electronic structure of the DWNT around the Fermi energy. E_g denotes the energy gap between the top of the valence and the bottom of the conduction bands, whereas E_g' denotes the energy gap between the lowest π^* states on the outer nanotube and the highest π state on the inner nanotube.

DWNT's are energetically unfavorable compared with two SWNT's. On the other hand, the inner tubes (7,0) and (12,0) give the largest energy gain for the outer tubes (15,0) and (20,0), respectively. Thus, it is plausible that the atomic arrangement of the inner tube is incommensurate with that of the outer tube under the energetically stable geometry and that the MWNT's exhibit the local AB ordering only in part of their wall. The calculations correspond to an experimental result in which the TEM image clearly shows such local ordering.

Figures 3(a)–3(d) show the electronic band structures of (5,0), (7,0), (9,0), and (15,0) BN nanotubes, respectively. All zigzag BN nanotubes are semiconducting with a direct energy gap at the Γ point. In the h-BN, the top of the valence band is at the K point which is folded into a Γ point in the zigzag BN tube.[10,11,24,25] Thus, the top of the valence band of the BN tube has π character distributed on N atomic sites. On the other hand, the bottom of the conduction band of the BN nanotube exhibits interesting variations: For the thick nanotube, (15,0), the bottom of the conduction band shows its nearly-free-electron (NFE) character,[11] which has the same characteristics as the bottom of the conduction band (the interlayer state) of h-BN at the Γ point.[24,25] For the thin

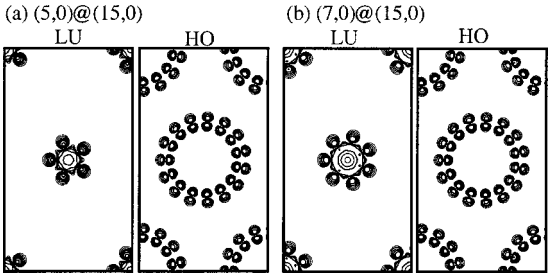

FIG. 4. Contour plots of the squared wave functions of Γ at the top of the valence band and the bottom of the conduction band on the cross-sectional plane of DWNT $(n,0)$@(15,0) for (a) $n=5$ and (b) $n=7$. "LU" and "HO" denote the lowest branch of the conduction band and the highest branch of the valence band, respectively. Each contour represents twice (or half) the density of the adjacent contour lines. The lowest value represented by the contour is 1.5625×10^{-4} $e/(\text{a.u.})^3$.

nanotubes, (5,0), (7,0), and (9,0), the conduction-band bottom does not show NFE character but shows π^* character which is mainly localized on the B atomic sites. The π^* states of thin nanotubes shift downward due to the hybridization between the π and σ states, which is originated from the large curvature of the thin tubes. In fact, the energy gap decreases with increasing curvature of the tubes: The calculated energy gaps of (5,0), (7,0), (9,0), and (15,0) tubes are 2.4 eV, 3.4 eV, 3.8 eV, and 4.4 eV, respectively.[26] The hybridization induces the downward shift not only for π^* states but also for π states. The shift is found to strongly depend on the tube radius, so that the electronic structure near the energy gap of BN DWNT's may show richer variation than that of the SWNT's.

Figures 3(e)–3(g) show the electronic band structures of BN DWNT's, (5,0)@(15,0), (7,0)@(15,0), and (9,0)@(15,0), respectively. All the systems are semiconducting with a direct energy gap at the Γ point as in the case of BN SWNT's. However, the energy gap of all DWNT's is slightly narrower than that of the inner nanotubes. The calculated gap energies are 1.7 eV, 2.9 eV, and 3.6 eV for (5,0)@(15,0), (7,0)@(15,0), and (9,0)@(15,0), respectively. This narrow gap is totally due to the difference in the downward shift of the π electron states between the inner and outer nanotubes: Downward shifts of the π states of the inner tube are larger than those of the outer tube. Thus, the top of the valence band is the π state of the outer tube, whereas the bottom of the conduction band is the π^* state of the inner tube [Fig. 3(h)]. The amplitude distribution of the wave function unequivocally reveals that the top of the valence band is distributed on the outer nanotube while the bottom of the conduction band is distributed on the inner nanotube (Fig. 4). The characteristics of the wave-function distribution imply that the BN DWNT's are applicable to the semiconductor-laser devices which can emit variable frequencies of laser depending on the direction of bias voltage or the site-controlled injection of carriers. When we apply the bias voltage along the direction from the inner tube to the outer tube, electrons and holes are injected into the inner and outer nanotubes, respectively. In this case, the DWNT emits violet light or ultraviolet rays between the energy gaps [E_g in Fig. 3(h)] of 2.9 eV for (7,0)@(15,0) and of 3.6 eV for (9,0)@(15,0).[26] On the contrary, by applying the inverse bias voltage from the outer to inner tube direction, the DWNT emits the ultraviolet rays between the lowest π^* state on the outer tube and the highest π state on the inner tube [E_g' in Fig. 3(h)], which has a shorter wavelength than that emitted between the highest occupied and the lowest unoccupied states.

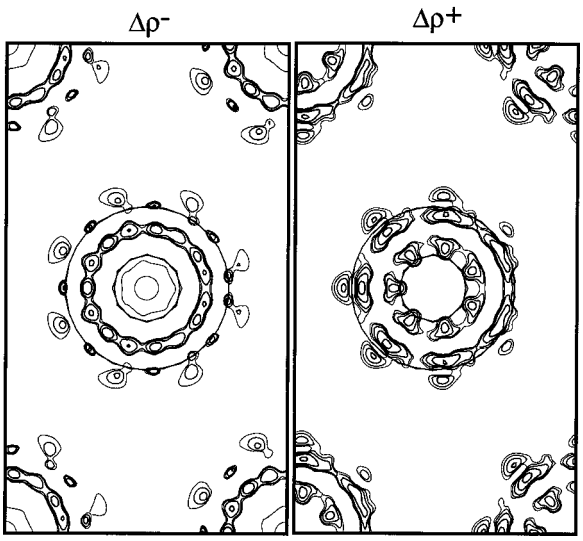

FIG. 5. The contour plots of the more negatively charged (electron-rich) area, $\Delta\rho^-$, and that of the more positively charged, $\Delta\rho^+$, area than a simple sum of self-consistent charge densities of the isolated SWNT's for a (7,0)@(15,0) BN DWNT. Circles denote the walls of inner and outer nanotubes. Each contour represents twice (or half) the density of the adjacent contour lines. The lowest value represented by the contour is 1.5625×10^{-4} $e/(\text{a.u.})^3$.

Finally, we discuss the self-consistent charge redistribution in the BN DWNT. In Fig. 5, we show the difference between the charge density of the DWNT and the sum of the charge densities of the isolated inner and the outer BN nanotubes, $\Delta\rho=\rho_{(n,0)@(m,0)}-(\rho_{(n,0)}+\rho_{(m,0)})$. It is clear that the electrons are transferred mainly from the π orbitals of both inner and outer BN nanotubes to the space between the tubes. Similar charge redistribution is also found in the carbon peapod,[27] the BNC peapod,[28] and double-walled carbon nanotubes.[29] The distribution of the electron-rich region $(\Delta\rho^-)$ is similar to that of the NFE states which is the common characteristic of tubular and layered materials, such as BN nanotubes,[11] carbon nanotubes,[30,31] graphite,[32,33] and h-BN.[24,25] It is known that the NFE state of the h-BN monolayer is located at about 5 eV above the top of the valence band and distributed about 2–3 Å above and below the sheet. In the BN tubes, the state exhibits concentric distribution and is extended along the tube axis.[11] The distribution of accumulated charge gives evidence of the hybridization between π states of the BN tube and the NFE state. It is noteworthy that the NFE states are still located at about 5 eV or more above the valence-band top and that the distribution is not the NFE state itself. However, we hardly detect which eigenstates of π electrons are dominantly hybridized with the NFE state. The charge redistribution observed has contributions from many π states not only near but also far below the NFE states.

In summary, we have studied the energetics and electronic structure of double-walled BN nanotubes. We found that the total energy of DWNT's has a local minimum around the interwall distance of about 3.0 Å: Under the optimum interwall distance, the index difference between the inner and outer nanotubes is 8 so that the most favorable DWNT is $(n,0)@(n+8,0)$. The electronic structure of the DWNT exhibits interesting variations around the energy gap. Owing to the large curvature of the BN nanotube which induces the hybridization between σ and π states of both tubes, the top of valence and the bottom of conduction bands are localized on the outer and inner nanotubes, respectively. It is expected that the peculiar character is applicable to the semiconductor-laser technology. We also found an interesting charge redistribution in the BN DWNT: The distribution of accumulated charge is corresponding to that of the NFE states of the BN nanotubes due to the hybridization between the NFE and π states.

We have benefited from conversations with D. Golberg and Y. Bando. Computations were done at the Institute for Solid State Physics, University of Tokyo, at the Science Information Processing Center, University of Tsukuba, and at the Research Center of Computational Science, Okazaki National Institute. This work was supported in part by JSPS under Contract No. RFTF96P00203, a Grant-in-Aid for Scientific Research, No. 11740219, and Grant No. 10184101 from the Ministry of Education, Science, and Culture of Japan.

[1] S. Iijima, Nature (London) **354**, 56 (1991).
[2] N.G. Chopra *et al.*, Science **269**, 966 (1995).
[3] D. Golberg *et al.*, Appl. Phys. Lett. **69**, 2045 (1996).
[4] W. Han *et al.*, Appl. Phys. Lett. **73**, 3085 (1998).
[5] D. Golberg *et al.*, Chem. Phys. Lett. **308**, 337 (1999).
[6] E. Bengu and L.D. Marks, Phys. Rev. Lett. **86**, 2385 (2001).
[7] D. Golberg *et al.*, Solid State Commun. **116**, 1 (2000).
[8] A. Zettle, *Abstracts of the Tsukuba Symposium on Carbon Nanotubes in Commemoration of the 10th Anniversary of Its Discovery* (Science Academy Tsukuka, Tsukuba, 2001), p. 10.
[9] D. Golberg *et al.*, Appl. Phys. Lett. **77**, 1979 (2000).
[10] A. Rubio, J. Corkill, and M.L. Cohen, Phys. Rev. B **49**, 5081 (1994).
[11] X. Blase *et al.*, Europhys. Lett. **28**, 335 (1994).
[12] N. Hamada, S. Sawada, and A. Oshiyama, Phys. Rev. Lett. **68**, 1579 (1992).
[13] R. Saito, *et al.*, Appl. Phys. Lett. **60**, 2204 (1992).
[14] P. Hohenberg and W. Kohn, Phys. Rev. **136**, B864 (1964).
[15] W. Kohn and L.J. Sham, Phys. Rev. **140**, A1133 (1965).
[16] J.P. Perdew and A. Zunger, Phys. Rev. B **23**, 5048 (1981).
[17] D.M. Ceperley and B.J. Alder, Phys. Rev. Lett. **45**, 566 (1980).
[18] N. Troullier and J.L. Martins, Phys. Rev. B **43**, 1993 (1991).
[19] L. Kleinman and D.M. Bylander, Phys. Rev. Lett. **48**, 1425 (1982).
[20] S. Okada *et al.*, Phys. Rev. B **62**, 9896 (2000).
[21] O. Sugino and A. Oshiyama, Phys. Rev. Lett. **68**, 1858 (1992).
[22] E. Hernandez *et al.*, Phys. Rev. Lett. **80**, 4502 (1998).
[23] R.W.G. Wychoff, *Crystal Structure* (Interscience, New York, 1965), Vol. 1.
[24] A. Catellani *et al.*, Phys. Rev. B **36**, 6105 (1987).
[25] X. Blase *et al.*, Phys. Rev. B **51**, 6868 (1995).
[26] The values of the calculated energy gaps have only qualitative meanings due to the limitation of the LDA.
[27] S. Okada, S. Saito, and A. Oshiyama, Phys. Rev. Lett. **86**, 3835 (2001).
[28] S. Okada, S. Saito, and A. Oshiyama, Phys. Rev. B **64**, 201303 (2001).
[29] Y. Miyamoto, S. Saito, and D. Tomanek, Phys. Rev. B **65**, 041402 (2002).
[30] Y. Miyamoto *et al.*, Phys. Rev. Lett. **74**, 2993 (1995).
[31] S. Okada, A. Oshiyama, and S. Saito, Phys. Rev. B **62**, 7634 (2000).
[32] M. Posternak, *et al.* Phys. Rev. Lett. **50**, 761 (1983).
[33] M. Posternak, *et al.* Phys. Rev. Lett. **52**, 863 (1984).